Compact Parameterization of Nonrepeating FMCW Radar Waveforms

Thomas J. Kramer[1], Erik R. Biehl[1], Matthew B. Heintzelman[1], Shannon D. Blunt[1], Eric D. Steinbach[2]
[1]Radar Systems Lab (RSL), University of Kansas, Lawrence, KS
[2]Sandia National Laboratories (SNL), Albuquerque, NM

***Abstract*—Spectrally shaped forms of random frequency modulation (RFM) radar waveforms have been experimentally demonstrated for a variety of implementation approaches and applications. Of these, the continuous-wave (CW) perspective is particularly interesting because it enables the prospect of very high signal dimensionality and arbitrary receive processing from a range/Doppler perspective, while also mitigating range ambiguities by avoiding repetition. Here we leverage a modification to the constant-envelope orthogonal frequency division multiplexing (CE-OFDM) framework, which was originally proposed for power-efficient communications, to realize a nonrepeating FMCW radar signal that can be represented with a compact parameterization, thereby circumventing memory constraints that could arise for some applications. Experimental loopback and open-air measurements are used to demonstrate this waveform type.**

Keywords—frequency modulation, CE-OFDM, noise radar, waveform diversity

I. Introduction

The choice of a particular waveform is a crucial decision that bears on the performance of a radar system. It is therefore no surprise that substantial work (e.g. see [1-4]) has focused on waveform optimization. Of course, there is also the matter of whether an optimized waveform can actually be implemented in radar hardware, with FM signals having sufficient spectral containment being particularly useful [4].

In contrast to identifying a single best waveform for a given application is the notion that the nonrepeating nature of randomness can instead realize the intrinsic benefits of high dimensionality. Noise radar [5,6] is the most well-known example of this waveform type, with FM noise or random FM (RFM) constituting versions suitable to high-power [7-10]. The class of spectrally-shaped RFM waveforms [10] address the Fourier relationship between power spectral density and autocorrelation, where maintaining low range sidelobes in the latter necessitates consideration of attributes in the former. Moreover, focus on spectral shape inherently contends with the need for containment to reduce (but never fully avoid) transmitter distortion effects.

A variety of different methods have thus far been developed and experimentally evaluated for spectrally-shaped RFM (see references in [10]), with new capabilities subsequently emerging such as cognitive sense-and-notch [11], physical realization of complementary waveforms [12], and intermodulation-based nonlinear radar [13]. Nearly all of these design approaches entail some degree of optimization, either on a per-pulse basis or to produce a waveform generating function [14]. A noteworthy exception is CE-OFDM, which was originally devised as a power and spectrally efficient scheme for communications [15-18] and later examined as a means of generating diverse radar waveforms [19-27] since it inherently possesses an FM structure. In [24] it was recognized that, when allowing CE-OFDM to produce distinct signals by randomizing the underlying symbols, it becomes an optimization-free form of spectrally-shaped RFM since the spectral density is naturally Gaussian via the central limit theorem.

Here we examine a subtle, yet meaningful modification to the CE-OFDM framework to undo the inherent periodic structure arising from the OFDM component. In so doing, yet another form of spectrally-shaped RFM is obtained that can produce a nonrepeating FMCW signal having an extremely compact parameterization. Consequently, this new form is an attractive prospect for applications in which memory storage and/or computational resources are at a premium.

II. Overview of CE-OFDM

The well-known OFDM signal structure, commonly used for commercial communications, can be defined as [4]

$$u(t) = \sum_{n=1}^{N} \beta_n \exp\left(j2\pi f_n t \right) \tag{1}$$

for symbol interval T, where β_n is the communication symbol (for some constellation, e.g. QAM) associated with subcarrier frequency f_n (of N), the collection of which are centered around zero at complex baseband. Orthogonality between subcarriers is achieved by setting the corresponding subcarrier frequencies such that they are separated by $1/T$. Clearly the superposition of these weighted subcarriers means that the amplitude envelope of $u(t)$ is not constant, with values for the ensuing peak-to-average power ratio (PAPR) commonly being on the order of 10-12 dB. While OFDM is attractive from an information capacity standpoint for communications, the presence of significant amplitude modulation (AM) requires linear amplification on transmit. Consequently, OFDM has limited utility for radar due to the collection of losses that generally necessitate use of a saturated high-power amplifier on transmit to maximize "energy on target", which introduces significant distortion when AM is present [28].

In the communication context, CE-OFDM was proposed [15-18] as a means to avoid the AM limitation (with attendant linear amplification) and associated poor power efficiency (noting that some hardware implementations can also perform

This work was supported in part by Sandia National Laboratories under Contract #2237007 and the Office of Naval Research under Contract #N00014-20-C-1006. This paper describes objective technical results and analysis. Any subjective views or opinions that might be expressed in the paper do not necessarily represent the views of the U.S. Department of Energy or the United States Government. DISTRIBUTION STATEMENT A. Approved for Public Release.

linearization at somewhat higher power efficiency [29]). In essence, CE-OFDM exponentiates the real part of OFDM via

$$s(t) = \exp\left(j2\pi h\, \mathbb{R}\{u(t)\}\right) = \exp\left(j2\pi\, \theta(t)\right) = \exp\left(j2\pi h \sum_{n=1}^{N} |\beta_n| \cos\left(2\pi f_n t + \phi_n\right)\right), \quad (2)$$

thereby realizing a form of FM, where the constant amplitude and continuous phase structure of FM signals make them naturally amenable to high-power amplification. Here h is the modulation index that scales the FM spectral content, $\mathbb{R}\{\bullet\}$ extracts the real part of the argument, $\theta(t)$ is the overall instantaneous phase, and $|\beta_n|$ and ϕ_n are the respective magnitude and phase of symbol β_n for $n = 1, 2, \ldots, N$.

This FM versus AM contrast means that (2) can be generated with higher power efficiency than (1). From a radar standpoint, (2) represents a physically meaningful signal structure with which to construct waveforms amenable to high-power transmitters. This capability has been examined in [19-27], and with new variants continuing to emerge under the auspices of multitone sinusoidal FM [30]. In [24], for each independent random symbol interval T separated into a distinct pulsed waveform, the nonrepeating nature of CE-OFDM was shown experimentally to realize a low-cost (i.e. optimization-free) form of RFM, where the independent range sidelobes on a pulse-to-pulse basis provide an incoherent averaging effect during slow-time combining. Here we examine a subtle modification to the CE-OFDM structure that eliminates periodicity, thereby facilitating nonrepeating FMCW operation.

III. Implications of Removing Periodicity

With the subcarrier frequencies in (1) and (2) separated by $1/T$, both signal structures are uniquely defined over the interval $[0, T]$, outside of which the signal repeats if the N values of β_n remain fixed. From a radar standpoint, removing such periodicity either mitigates range ambiguities or avoids large range sidelobes, depending on whether one is performing slow-time or fast-time processing, respectively.

Obviously, periodicity would not occur if the set of β_n values were changed each subsequent T interval. However, the nature of the symbol change must be addressed to avoid phase discontinuities that incur spectral spreading and distortion to the amplitude envelope in the same manner as phase codes (see [31]). It is for this reason that radar consideration of CE-OFDM has set symbol interval T to likewise be the pulse width.

Extending this pulsed framework to realize a nonrepeating CW waveform within the CE-OFDM context suggests that we should reconsider the signal structure itself. To do so, write the subcarrier frequencies from (2) in the incremental form

$$f_n = f_1 + (n-1)/T = f_{n-1} + 1/T \quad (3)$$

for $n = 1, 2, \ldots, N$, which clearly illustrates the frequency differences are integer multiples of $1/T$ (top line) and the difference between adjacent subcarriers is $1/T$ (bottom line). It is the relationship between these frequencies that we shall revisit, but first a quick review of periodicity.

In general, it is well-known that for any sum of periodic functions (e.g. sinusoids) the period of the sum is equal to the least common multiple (LCM) of the individual periods. In short, if $a(t)$ and $b(t)$ are two such periodic functions, then $a(t) = a(t + kT_a)$ and $b(t) = b(t + \ell T_b)$ for T_a and T_b their respective periods and with k and ℓ integers. Therefore, the summation $c(t) = a(t) + b(t)$ is likewise periodic with $c(t) = c(t + mT_{\text{LCM}})$ for integer m and period $T_{\text{LCM}} = kT_a = \ell T_b$ for whatever are the smallest positive integer values of k and ℓ, i.e. the LCM of T_a and T_b.

Denoting the inverse of the LCM period as the frequency $f_{\text{LCM}} = 1/T_{\text{LCM}}$, and likewise $f_a = 1/T_a$ and $f_b = 1/T_b$, it is easy to see that $(k \times f_{\text{LCM}}) = f_a$ and $(\ell \times f_{\text{LCM}}) = f_b$. In other words, the frequencies f_a and f_b are integer multiples of f_{LCM}, with a direct extension to multiple frequencies that meet this criterion while ensuring the LCM period remains unchanged. Moreover, we see that their ratio is $f_a / f_b = k / \ell$, which is a rational number. Clearly, we have just described the OFDM framework that is likewise used in CE-OFDM.

Since we are interested in FM waveforms specifically, let T_{CE} denote the period for CE-OFDM in (2), which again is the same as OFDM. Accounting for negative frequencies at complex baseband, we can therefore denote

$$T_{\text{CE}} = \text{LCM}\left\{\frac{1}{|f_1|}, \frac{1}{|f_2|}, \cdots, \frac{1}{|f_N|}\right\} \quad (4)$$

excluding $f_n = 0$, with the frequencies selected to be integer multiples of $1/T_{\text{CE}}$ to maintain a fixed period. Indeed, from the standpoint of information capacity within the communication context, it is generally desired for this period to be as short as possible so that as many symbols can be conveyed within a given time interval, i.e. maximize data rate.

However, if our goal is instead to realize a nonrepeating CW waveform that has utility in the radar context, we wish to minimize correlation between different portions of the CW signal that would otherwise introduce range ambiguities or range sidelobes (depending on slow-time or fast-time perspective). Consequently, we now seek to maximize the period resulting from the LCM of the constituent frequencies.

As it turns out, it is straightforward to produce a signal based on the general CE-OFDM structure of (2) that in fact never repeats. Noting the previous statement that the ratio of CE-OFDM frequencies produces a rational number, all we need to do is select frequencies such that f_a / f_b is irrational. Put another way, now set

$$f_n = f_{n-1} + (1 + \alpha_n)/T \quad (5)$$

given f_1, letting each α_n for $n = 2, 3, \ldots, N$ be a unique, irrational, real number with $|\alpha_n| << 1$. Consequently, each ratio

$$\frac{f_n}{f_{n-1}} = \frac{f_{n-1} + (1+\alpha_n)/T}{f_{n-1}} = 1 + \frac{1}{f_{n-1}T} + \frac{\alpha_n}{f_{n-1}T} \quad (6)$$

is likewise irrational. In short, we select $(N-1)$ subcarrier spacings that are irrational (as opposed to being integers) and so refer to this form as non-integer constant-envelope OFDM, or NICE-OFDM (though the OFDM designation is no longer precisely true). The application of (4) with these irrationally

related subcarriers therefore yields $T_{\text{NICE}} \to \infty$ (assuming all irrational components are unique).

Moreover, note that the span of N subcarriers in (3) is

$$f_N - f_1 = (N-1)/T\,. \tag{7}$$

The same general subcarrier span can be realized for NICE-OFDM using (5) when

$$(N-1) \approx \sum_{n=2}^{N}(1+\alpha_n) = (N-1) + \sum_{n=2}^{N}\alpha_n \tag{8}$$

with the summation over α_n being approximately zero if we assume a uniform distribution on small interval $[-\delta, +\delta]$, and after removing the common $1/T$ component. Therefore, along with N arbitrary symbols β_n, a set of $(N-1)$ irrational subcarrier spacings is the only parameterization required to produce an FM signal that never repeats, yet is completely known. In fact, the β_n terms can be ignored as well (e.g. set =1) if non-repetition is the only goal, though we shall retain them for generality.

It was noted in [24] based on work in [16,32,33] that the CE-OFDM form in (2) can likewise be expressed using the Jacobi-Anger expansion as

$$s(t) = \prod_{n=1}^{N}\sum_{m=-\infty}^{\infty} d_{n,m}\, \exp\left(j2\pi m f_n t\right) \operatorname{rect}\left(\frac{t - T_{\text{CE}}/2}{T_{\text{CE}}}\right) \tag{9}$$

for coefficients

$$d_{n,m} = j^m J_m\left(2\pi h\left|\beta_n\right|\right) \exp\left(jm\phi_n\right), \tag{10}$$

with $J_m(\bullet)$ the mth Bessel function of the first kind and the rect(•) function denoting pulsed time support on $[0, T_{\text{CE}}]$. The Fourier transform of each weighted infinite sum in (9) becomes a similarly weighted infinite sum of sinc(•) functions in the frequency domain (due to the rect(•) function), with each term centered at mf_n. Consequently, since the N-fold repeated product in (9) becomes a repeated convolution in frequency, the overall result via the central limit theorem (CLT) causes $s(t)$ to tend toward a Gaussian spectral density on average, given sufficiently large N and h.

In regard to the NICE perturbation of subcarrier spacing via (5), one could surmise that the sinc(•) functions noted above collapse to impulses since we are replacing T_{CE} with $T_{\text{NICE}} \to \infty$. However, because practical radar operation still only occurs during a finite interval, the repeated convolution of an infinite number of frequency-domain sinc(•) functions likewise still applies, implying the spectral density (on average) remains Gaussian since the frequency span via (8) and number of subcarriers N are fixed. Of course, a given waveform instantiation could deviate somewhat from this form, especially if the irrational α_n terms were to become large, and thus highly non-uniform. It is for this reason we have imposed $|\alpha_n| << 1$.

From a finite receive processing standpoint, denote T_{CPI} as a coherent processing interval (CPI) that is segmented into M equal-length intervals T_{seg}. Per [34], some degree of overlap between adjacent segments is needed to account for convolutional tails when performing pulse compression, after which standard Doppler processing can be employed. Due to the nonrepeating nature of the waveform across the CPI, a clutter range sidelobe modulation (RSM) effect occurs just like with other RFM and noise signals [10]. An additional factor in this context arises when considering the instantaneous frequency, which is obtained from (2) as

$$f_{\text{inst}}(t) = \frac{d}{dt}\{\theta(t)\} = -2\pi h \sum_{n=1}^{N}\left|\beta_n\right| f_n \sin\left(2\pi f_n t + \phi_n\right). \tag{11}$$

Specifically, where CE-OFDM could include a (complex baseband) subcarrier at $f_n = 0$, irrational perturbation via α_n could realize a $f_n \neq 0$ that is nonetheless small. If the inverse of this particular subcarrier roughly lies within $T_{\text{CPI}} > 1/f_n > T_{\text{seg}}$, and N is not sufficiently large for the contribution of any single subcarrier to be disregarded, then (11) exhibits what appears to be a drift in center frequency across the segments of the CPI. While arising from a different cause (i.e. varying locations of spectral notches), this modulation of center frequency over the CPI can exacerbate the effects of clutter modulation [11].

Another important impact of instantaneous frequency arises when the collection of terms in (11) combines to produce a value for $f_{\text{inst}}(t)$ that is sufficiently large relative to the "over-sampling" used to discretize the signal for implementation (e.g. on an arbitrary waveform generator). In such cases, the discretized form of the FM signal becomes distorted because it cannot "keep up" with the rate of phase-change, resulting in a degree of AM emerging from the necessary "shorter path" through the unit phase circle (instead of around the circle). Given the Gaussian spectral density due to the CLT, combined with a practical trade-off for sample rate, such outlier frequencies are essentially guaranteed. Of course, abrupt phase changes like in the CE-OFDM case (CW version) produce more extreme distortion, which we observe in Sect. V.

Finally, while the period of repetition can theoretically be driven to $T_{\text{NICE}} \to \infty$ by the use of irrational subcarrier spacings, this condition really just means that a perfect replica of one portion of the signal is not reproduced elsewhere. However, that does not mean that some relatively high sidelobe could not occur. While the complete avoidance of a higher sidelobe cannot be guaranteed, the likelihood (or severity) can clearly be reduced by simply increasing the number N of irrationally spaced subcarriers, thereby increasing the complexity of the signal, and thereby reducing the prospect of higher similarity.

IV. Hardware Loopback Examples

To illustrate the benefit of non-repetition, two 100 ms waveforms (one CE-OFDM and one NICE-OFDM) were generated to have a 50 MHz 3-dB bandwidth that is oversampled by 4 (i.e. 200 MHz sample rate). Each waveform was constructed from $N = 200$ subcarriers using a fixed set of β_n symbols randomly drawn from a 16-QAM constellation.

For the first waveform, a uniform subcarrier spacing is set to 10 kHz, corresponding to a repetition period of $T_{\text{CE}} = 100$ μs. Consequently, the signal repeats 1000 times over the 100 ms interval. Note that no phase discontinuities occur at the transition between symbol intervals because this form is simply allowing (2) to extend in time beyond the nominal period.

The $N - 1 = 199$ values of α_n for the NICE-OFDM waveform were randomly generated by a uniform distribution within ±1 kHz. Here, the minimum subcarrier frequency was 10 kHz and the maximum subcarrier frequency was 2 MHz

(note that the actual bandwidth is only loosely dependent on these values since subcarriers are exponentiated and scaled by h). While random assignment does not necessarily ensure the α_n terms are irrational, for sufficiently large N the end result is indistinguishable.

Using waveform versions captured in hardware loopback, Figs. 1 and 2 illustrate the respective autocorrelations for uniform and non-uniform subcarrier spacing, with the former clearly showing a repetitive structure, which is unsurprising since the symbols are fixed. In contrast, the latter reveals a peak sidelobe level of –58 dB, which is about an order of magnitude shy of the $-10\log_{10}(TB) = -67$ dB benchmark when using $TB = (100\times10^{-3})(50\times10^{6}) = 5\times10^{6}$.

Fig. 3 plots the loopback-captured autocorrelation for standard use of CE-OFDM in which the 1000 symbol intervals contain variable random symbols (independently drawn from 16-QAM for each subcarrier and interval). Here a peak sidelobe level of –58 dB is likewise realized, yet doing so entails a 1000× increase in data representation and also incurs phase discontinuities at transitions between symbol intervals.

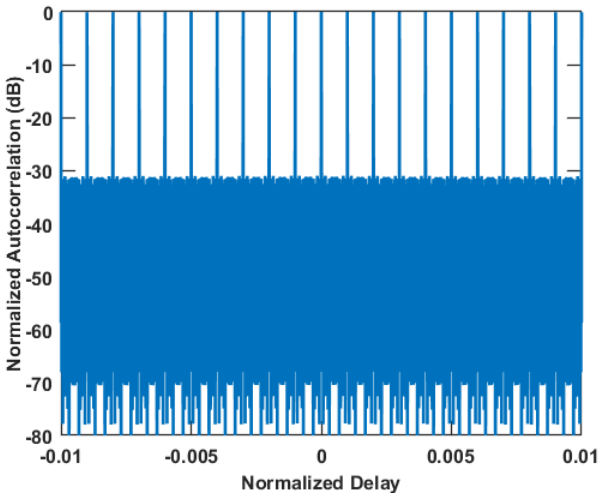

Fig. 1. Autocorrelation of a 100ms "fixed symbols" CE-OFDM signal possessing 1000 repeated symbol intervals (zoomed-in view)

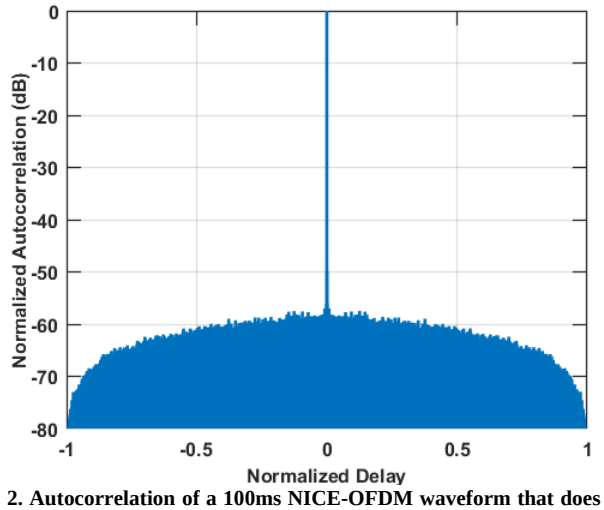

Fig. 2. Autocorrelation of a 100ms NICE-OFDM waveform that does not repeat, despite the symbols remaining fixed

While Figs. 1-3 illustrate the degree of self-similarity over the entire waveform, segment-wise receive processing is likely to be more appropriate for most applications. Therefore, Fig. 4 shows the "per-segment" auto/cross-correlations averaged over $M = 1000$ segments (so $T_{seg} = 100$ μs) for NICE-OFDM, where each segment corresponds to $T_{seg}B = (1\times10^{-4})(50\times10^{6}) = 5\times10^{3}$ so the associated $-10\log_{10}(T_{seg}B) = -37$ dB benchmark is close to the RMS average peak autocorrelation sidelobe of –39 dB in Fig. 4. We also see the cross-correlation peak is –42 dB. Slow-time combining (Doppler processing) of these segment-wise responses would realize a sidelobe level on par with Fig. 2.

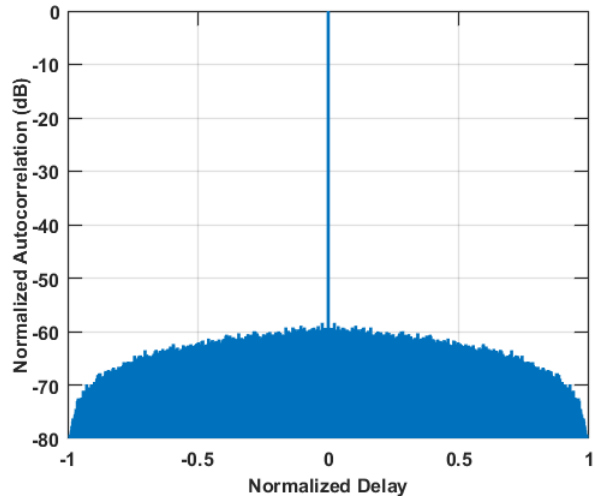

Fig. 3. Autocorrelation of a 100ms "variable symbols" CE-OFDM signal with 1000 independent (nonrepeating) symbol intervals

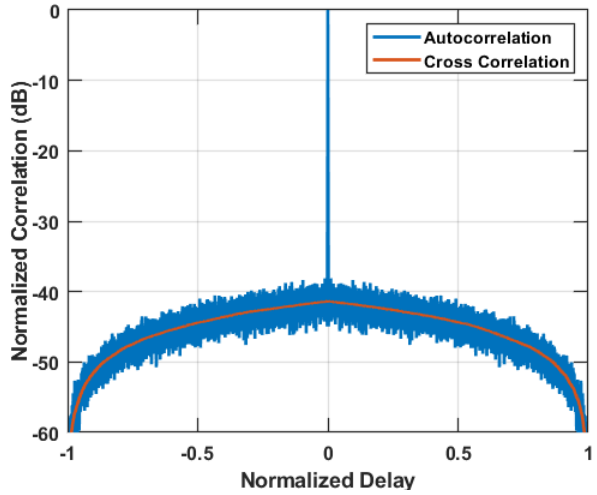

Fig. 4. Per-segment RMS average of autocorrelation and cross-correlation for 1000 unique segments of NICE-OFDM (each segment is 100 μs)

V. Experimental Results

To experimentally demonstrate the utility and trade-space of nonrepeating CW signals such as NICE-OFDM, open-air measurements at 3.45 GHz were collected from the roof of Nichols Hall at the University of Kansas (see [10] for description of test setup). Vehicles moving north and south were illuminated crossing the intersection of 23rd and Iowa streets, about a kilometer from the rooftop.

The same 50 MHz / 100 ms waveform classes as above were transmitted (excluding the range-ambiguous case). Here the CW signals were separated into 10^4 segments of 10 µs each to form pulse compression filters (including some before/after portion of each to account for convolutional tails [34]). For the sake of computational efficiency, Doppler processing and clutter cancellation was performed using every 100th captured segment in a quasi-pulsed manner that emulates a pulse repetition interval (PRF) of 1 kHz and 100 "pulses". This approach was repeated 100 times using each offset collection of 100 pulse-like segments. The resulting set of 100 range/Doppler responses (still complex) was then combined via averaging.

Since CW operation also tends to necessitate separate transmit and receive antennas, direct path leakage must also be addressed so that meaningful receive sensitivity is obtained. We used a version of the CLEAN method (see [35]) that also accounts for range straddling. Clutter cancellation involved simple projection-based suppression at/around zero Doppler (since the platform is stationary).

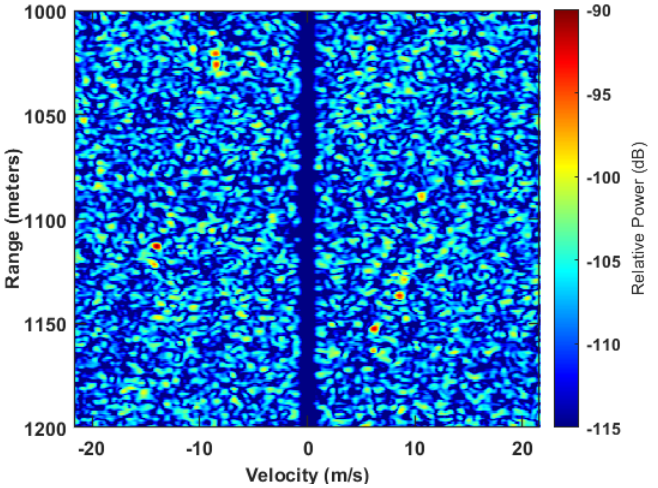

Fig. 5. Range-Doppler response for $M = 10^4$ segments of NICE-OFDM that has random subcarrier offsets and does not repeat

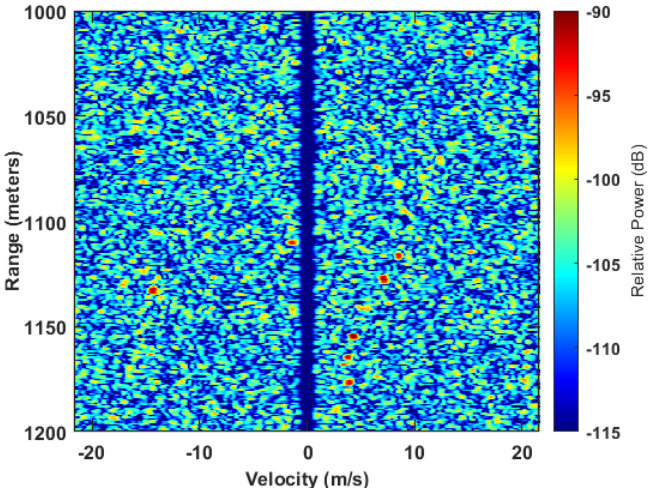

Fig. 6. Range-Doppler response for $M = 10^4$ unique segments of a "variable symbols" CE-OFDM signal that has uniform spacing and changes symbols every 100 µs

This test setup and processing arrangement was used for both a NICE-OFDM signal like in Fig. 2 and a "variable symbols" version of CE-OFDM like in Fig. 3, neither of which repeat. These open-air captures were performed consecutively, so while the disposition of movers is not identical, the scene and hardware similarity are sufficient to permit qualitative comparison.

Fig. 5 shows the NICE-OFDM result in which several movers are observed relative to the background after clutter cancellation. Fig. 6 depicts a similar result for the "variable symbols" version of CE-OFDM, albeit with a moderately higher background floor. The reason for the higher background can be understood when examining Fig. 7 that depicts the complex samples of each signal (loopback version), where we observe the "shorter paths" through the unit phase circle that each waveform takes (ideally both would only lie on the circle). The NICE-OFDM deviation from the circle results from only "over-sampling" the discretized representation by 4 (relative to 3-dB bandwidth), while the more severe distortion of CE-OFDM is due partly to this same effect, but is mainly due to abrupt phase transitions between symbols (hence traversals across the center). The sampling issue can be addressed by higher discretization rate (or perhaps imposing further spectral shaping within the FM structure). Eliminating abrupt phase transitions could, in general, be addressed with a structure like continuous phase modulation (CPM), such as developed in [31] for radar applications, though it is not clear how that structure would be incorporated into the CE-OFDM framework.

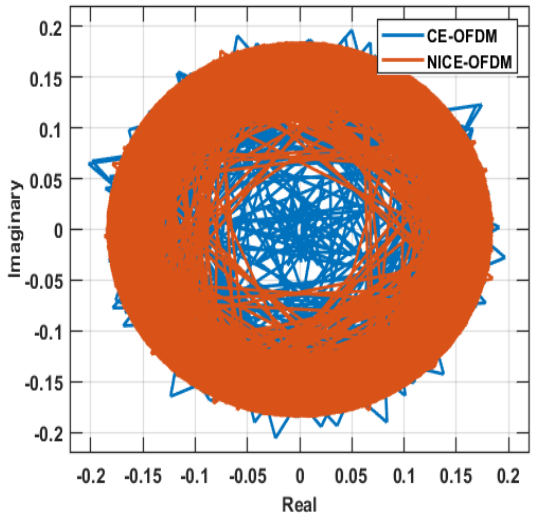

Fig. 7. Plot of the complex signal samples for NICE-OFDM and "variable symbols" CE-OFDM after loopback capture, illustrating the relative distortion each incurs in this implementation (4× over-sampled based on 3-dB bandwidth). Ideally each would remain on the unit phase circle.

VI. Conclusions

The nonrepeating nature of NICE-OFDM waveforms has been shown to provide a computationally-light, compact representation of a random FMCW signal having spectral characteristics that achieve low range sidelobes. Given sufficient transmit/receive isolation, this CW instantiation therefore facilitates easy generation of radar signals that may ultimately be useful in congested spectral environments since

they exhibit lower peak power (for the same "energy on target"), while providing high dimensionality for separability from increasingly ubiquitous interference.

REFERENCES

[1] M. Wicks, E. Mokole, S. Blunt, V. Amuso, R. Schneible, eds., *Principles of Waveform Diversity & Design*, SciTech Publishing, 2010.

[2] S. Pillai, K. Y. Li, I. Selesnick, B. Himed, *Waveform Diversity: Theory & Applications*, McGraw-Hill, 2011.

[3] F. Gini, A. De Maio, L. K. Patton, *Waveform Design and Diversity for Advanced Radar Systems*, IET Press, 2012.

[4] S.D. Blunt, E.L. Mokole, "An overview of radar waveform diversity," *IEEE Aerospace & Electronic Systems Mag.*, vol. 31, no. 11, pp. 2-42, Nov. 2016.

[5] B.M. Horton, "Noise-modulated distance measuring systems," *Proc. IRE*, vol. 47, no. 5, pp. 821-828, May 1959.

[6] S.R.J. Axelsson, "Random noise radar/sodar with ultrawideband waveforms," *IEEE Trans. Geoscience & Remote Sensing*, vol. 45, no. 5, pp. 1099-1114, May 2007.

[7] T.B. Whiteley, D.J. Adrian, "Random FM autocorrelation fuze system," U.S. Patent #4,220,952, issued 2 Sept. 1980, filed 17 Feb. 1956.

[8] S.R.J. Axelsson, "Noise radar using random phase and frequency modulation," *IEEE Trans. Geoscience & Remote Sensing*, vol. 42, no. 11, pp. 2370-2384, Nov. 2004.

[9] L. Pralon, B. Pompeo, J.M. Fortes, "Stochastic analysis of random frequency modulated waveforms for noise radar systems," *IEEE Trans. Aerospace & Electronic Systems*, vol. 51, no. 2, pp. 1447-1461, Apr. 2015.

[10] S.D. Blunt, et al., "Principles & applications of random FM radar waveform design," *IEEE Aerospace & Electronic Systems Mag*., vol. 35, no. 10, pp. 20-28, Oct. 2020.

[11] B. Ravenscroft, J.W. Owen, J. Jakabosky, S.D. Blunt, A.F. Martone, K.D. Sherbondy, "Experimental demonstration and analysis of cognitive spectrum sensing & notching," *IET Radar, Sonar & Navigation*, vol. 12, no. 12, pp. 1466-1475, Dec. 2018.

[12] C.C. Jones, C.A. Mohr, P.M. McCormick, S.D. Blunt, "Complementary frequency modulated radar waveforms and optimised receive processing," *IET Radar, Sonar & Navigation*, vol. 2021, no. 15, pp. 708-723, Apr. 2021.

[13] J. Owen, S.D. Blunt, K. Gallagher, P. McCormick, C. Allen, K. Sherbondy, "Nonlinear radar via intermodulation of FM noise waveform pairs," *IEEE Radar Conf.*, Oklahoma City, OK, Apr. 2018.

[14] C.A. Mohr, S.D. Blunt, "Design and generation of stochastically defined pulsed FM noise waveforms", *Intl. Radar Conf.*, Toulon, France, Sept. 2019.

[15] C.-D. Chung, S.-M. Cho, "Constant-envelope orthogonal frequency division multiplexing modulation", *Proc. APCC/OECC*, Beijing, China, Oct. 1999.

[16] S.C. Thompson, A.U. Ahmed, J.G. Proakis, J.R. Zeidler, "Constant envelope OFDM phase modulation: spectral containment signal space properties and performance," *IEEE Military Communications Conf.*, Monterey, CA, Oct./Nov. 2004.

[17] S.C. Thompson, et al., "Constant envelope OFDM", *IEEE Trans. Communications*, vol. 56, no. 8, pp. 1300-1312, Aug. 2008.

[18] M.P. Wylie-Green, E. Perrins, T. Svensson, "Introduction to CPM-SC-FDMA: a novel multi-access power-efficient transmission scheme", *IEEE Trans. Communications*, vol. 59, no. 7, pp. 1904-1915, July 2011.

[19] J.P. Stralka, "Applications of orthogonal frequency-division multiplexing (OFDM) to radar," Johns Hopkins University, PhD dissertation, Mar. 2008.

[20] R. Mohseni, A. Sheikhi, M.A. Masnadi Shirazi, "Constant envelope OFDM signals for radar applications," *IEEE Radar Conf.*, Rome, Italy, May 2008.

[21] S.C. Thompson, J.P. Stralka, "Constant envelope OFDM for power-efficient radar and data communications," *Intl. Waveform Diversity & Design Conf.*, Kissimmee, FL, Feb. 2009.

[22] S. Liu, Z. Huang, W. Zhang, "A power-efficient radar waveform compatible with communication," *Intl. Conf. Communications Circuits & Systems*, Chengdu, China, Nov. 2013.

[23] Q. Zhang, et al., "Waveform design for a dual-function radar-communication system based on CE-OFDM-PM signal," *IET Radar Sonar & Navigation*, vol. 13, no. 4, pp. 566-572, Apr. 2019.

[24] E.R. Biehl, C.A. Mohr, B. Ravenscroft, S.D. Blunt, "Assessment of constant envelope OFDM as a class of random FM radar waveforms", *IEEE Radar Conf*., Florence, Italy, Sept. 2020.

[25] B. White, M. Heintzelman, S.D. Blunt, "Alternative "bases" for gradient-based optimization of parameterized FM radar waveforms," *IEEE Radar Conf.*, San Antonio, TX, May 2023.

[26] D.G. Felton, D.A. Hague, "Gradient-based optimization of constant envelope OFDM waveforms," *IEEE Radar Conf.*, San Antonio, TX, May 2023.

[27] D.G. Felton, D.A. Hague, "Characterizing the ambiguity function of the constant-envelope OFDM waveforms," *IEEE Radar Conf.*, San Antonio, TX, May 2023.

[28] J. Jakabosky, L. Ryan, S.D. Blunt, "Transmitter-in-the-loop optimization of distorted OFDM radar emissions," *IEEE Radar Conf*., Ottawa, Canada, Apr./May 2013.

[29] F.H. Raab, P. Asbeck, S. Cripps, P.B. Kenington, Z.B. Popovic, N. Pothecary, J.F. Sevic, N.O. Sokal, "Power amplifiers and transmitters for RF and microwave," *IEEE Trans. Microwave Theory & Techniques*, vol. 50, no. 3, pp. 814-826, Mar. 2002.

[30] D.A. Hague, "Adaptive transmit waveform design using multitone sinusoidal frequency modulation," *IEEE Trans. Aerospace & Electronic Systems*, vol. 57, no. 2, pp. 1274-1287, April 2021.

[31] S.D. Blunt, M. Cook, J. Jakabosky, J. de Graaf, E. Perrins, "Polyphase-coded FM (PCFM) radar waveforms, part I: implementation," *IEEE Trans. Aerospace & Electronic Systems*, vol. 50, no. 3, pp. 2218-2229, July 2014.

[32] D.A. Hague, P. Kuklinski, "Waveform design using multi-tone feedback frequency modulation," *IEEE Radar Conf*., Boston, MA, Apr. 2019.

[33] M. Abramowitz, I.A. Stegun, *Handbook of Mathematical Functions with Formulas, Graphs, and Mathematical Tables*, US Dept. of Commerce, 1964, Chap. 9.

[34] J. Jakabosky, S.D. Blunt, B. Himed, "Waveform design and receive processing for nonrecurrent nonlinear FMCW radar," *IEEE Intl. Radar Conf*., Washington, DC, May 2015.

[35] K. Kulpa, "The CLEAN type algorithms for radar signal processing," *Microwaves, Radar & Remote Sensing Symp.*, Kiev, Ukraine, Sept. 2008.